J Solid State Electrochem (2011) 15:539–548
DOI 10.1007/s10008-010-1095-8

ORIGINAL PAPER

Facile electrosynthesis and thermoelectric performance of electroactive free-standing polythieno[3,2-*b*]thiophene films

Ruirui Yue · Shuai Chen · Baoyang Lu · Congcong Liu · Jingkun Xu

Received: 24 February 2010 / Revised: 13 April 2010 / Accepted: 5 May 2010 / Published online: 18 June 2010

Abstract Polythieno[3,2-*b*]thiophene (PTT) was electrosynthesized by facile anodic oxidation of thieno[3,2-*b*]thiophene (TT) in three systems: boron trifluoride diethyl etherate (BFEE), acetonitrile (ACN), and dichloromethane solutions. The onset oxidation potential of TT in BFEE was determined to be 0.62 V vs. Ag/AgCl, which was much lower than those in ACN and dichloromethane solutions. PTT films exhibited excellent electrochemical property, high thermal stability, good redox activity, and stability. Free-standing PTT films with good mechanical property can be obtained from BFEE solution, whose structure and morphology were characterized by FT-IR, UV–visible spectra, and scanning electron microscopy. With an electrical conductivity of 1.5 $S cm^{-1}$ and a Seebeck coefficient of 85 $\mu V K^{-1}$ at 306 K, the as-prepared free-standing PTT films showed a certain thermoelectric property. The dimensionless figure-of-merit of PTT films was estimated to be 2.3×10^{-3} at 306 K, which was much higher than those of some organic thermoelectric materials reported previously. All these results indicated that PTT films may have potential applications in the thermoelectric field.

Keywords Conducting polymers · Thieno[3,2-*b*]thiophene · Electrochemical polymerization · Thermoelectric property · Polythiophene

R. Yue · S. Chen · B. Lu · C. Liu · J. Xu (✉)
Jiangxi Key Laboratory of Organic Chemistry,
Jiangxi Science and Technology Normal University,
Nanchang 330013, China
e-mail: xujingkun@tsinghua.org.cn
e-mail: xujingkun@mail.ipc.ac.cn

Introduction

After the discovery of conductive polyacetylene in 1977 [1, 2], conjugated polymers have been well known for their interesting electrical and optical properties [3]. Since then, the synthesis of novel conjugated polymers with sophisticated properties and the exploration for new wider application fields for the already intensively investigated conducting polymers have been a subject of current intense research. Among the most extensively studied conjugated materials, oligomers and polymers containing thiophene units have received considerable attention because of their relatively good environmental stability, excellent electrical and optical properties, and tunability at the molecule level [4–6]. Thieno[3,2-*b*]thiophene (TT), with two condensed thiophene rings, has been investigated mainly by chemical oxidation, and the as-formed oligomers or polymers based on TT have attracted much attention because of their very rigid backbone which leads to good packing, high charge mobility, and high thermal stability [7–11]. However, few attentions have been focused on the electropolymerization of TT and properties of polythieno[3,2-*b*]thiophene (PTT) [12–15].

As well known, conjugated polymers can be synthesized chemically or electrochemically. Electrochemical polymerization has been proved to be one of the most useful approaches for conducting polymer synthesis with several advantages [16–22]. Firstly, one-step conducting film can be formed on the working electrode. Secondly, the amount of the polymer deposited on the electrode can be controlled by the integrated charge passed through the cell. Thirdly, only small amounts of monomer are required. Lastly, electrochemical studies can give fast information on the properties of electropolymerized materials with good accuracy and precision. However, the solvent chosen is a very important factor during the electrosynthesis of con-

ducting polymers [23]. According to the literature reported previously, conducting polymer films with high quality can be easily prepared in boron trifluoride diethyl etherate (BFEE) or its mixed electrolytes [17–22], mainly because of its good ionic conductivity and catalyst effect on the electropolymerization process of aromatic monomers, which make polymerizations of these monomers occur at lower potentials. Under this circumstance, BFEE serves not only as the solvent but also as the supporting electrolyte and no other supporting electrolyte is needed. In general, conducting polymer films electrodeposited from BFEE exhibit good electrical or optical properties, which will be of great benefit to their applications in electronic devices.

On the other hand, besides the extensively studied applications in sensors, polymeric light-emitting diodes, polymeric field-effect transistors, and photovoltaic cells [24–28], the novel and potential applications of conjugated materials in thermoelectric power generators and Peltier coolers, have also attracted much attention in recent years [29–34]. The efficiency of a thermoelectric material is related to the so-called dimensionless thermoelectric figure-of-merit (*ZT*) as defined by Eq. 1:

$$ZT = \frac{(S^2\sigma)T}{\kappa} \quad (1)$$

where S is the Seebeck coefficient, σ is the electrical conductivity, T is the absolute temperature, and κ is the thermal conductivity. A good thermoelectric material has a high *ZT* value at the operating temperature. The conventional thermoelectric materials are inorganic thermoelectric materials, which have mainly been investigated and developed at present, such as bismuth telluride [35–39]. However, the inorganic thermoelectric materials involve some issues such as toxicity, a shortage of natural resources, and complicated manufacturing processes with high cost [40, 41], while organic polymers are considered to be suitable for widespread use in applications because of the potentially low cost due to an abundance of carbon resources, easy synthesis in general, and easy processing into versatile forms [42–46]. Moreover, their low thermal conductivity is generally expected to be advantageous in enhancing thermoelectric properties [40]. Based on the above, some organic polymers and copolymers with relatively better thermoelectric properties have been reported in recent years, such as poly(2,5-dimethoxyphenylenevinylene) [40], copolymer of phenylenevinylene and dialkoxyphenylenevinylene [41], poly(2,7-carbazole) derivatives [42, 43], polycarbazole, polyindolocarbazole and polydiindolocarbazole derivatives [44], poly(3-octylthiophene)/silver nanocomposites [45], and poly(3,4-ethylenedioxythiophene)/poly(4-styrenesulfonate) (PEDOT/PSS) [46], etc. However, the study on the thermoelectric property of PTT has never been reported. Furthermore, according to the literature, there are significant improvements of the Seebeck coefficient of polydiindolocarbazole and its derivatives compared with those of polyindolocarbazole and polycarbazole, as the fused rings of the monomer increased [44]. Thus, it was expected that the Seebeck coefficient of PTT might be higher than that of polythiophene (PT) because of the extended π-conjugated structure.

In this paper, we synthesized TT according to the literature procedures [47] (Scheme 1). Then, TT has been electropolymerized in BFEE, acetonitrile (ACN) + 0.1 mol L^{-1} tetrabutylammonium tetrafluoroborate (Bu_4NBF_4), and CH_2Cl_2 + 0.1 mol L^{-1} Bu_4NBF_4 solutions, respectively. Comparative experiments have been carried out to optimize the proper electropolymerization system for TT. The electrochemical property, spectral characterization, thermal stability, and morphologies of the obtained PTT films were studied, respectively. The thermoelectric property of the obtained free-standing PTT films from BFEE was also investigated on.

Experimental details

Chemicals

BFEE (AR, Beijing Changyang Zhenxing Chemical Plant, China), commercial high-performance liquid chromatography-grade acetonitrile (AR, Beijing East Longshun Chemical Plant, China), dichloromethane, tetrahydrofuran (THF), and *N*,*N*-dimethylformamide (DMF, AR, Beijing Chemical Plant, China) were distilled before use. Concentrated sulfuric acid (AR, Ji'nan Chemical Reagent Company, China), diisopropylamine, *N*-formylpiperidine, and ethyl 2-sulfanylacetate (AR, Shanghai Zhuorui Chemical Plant, China), *n*-butyllithium (Shangyu Hualu Chemical Co., Ltd., Zhejiang, China), NH_4Cl (AR, Beijing Chemical Plant, China), quinoline (AR, Beijing Xizhong Chemical Plant, China), K_2CO_3 and $LiOH{\cdot}H_2O$ (AR, Tianjin Hengxing Reagents Factory, China), and copper powder (99.5%, AR, Tianjin Bodi Chemical Co., Ltd., China) were all used without further purification. Bu_4NBF_4 (98%) was purchased from J&K Chemical Ltd and dried in vacuum at 60°C for 24 h before use.

Electrochemical examination

Electrochemical polymerization and examination were carried out in a one-compartment three-electrode cell with a Model 263 potentiostat–galvanostat (EG&G Princeton Applied Research) under computer control at room temperature. The working and counter-electrodes for cyclic voltammetry (CV) experiments were two platinum wires

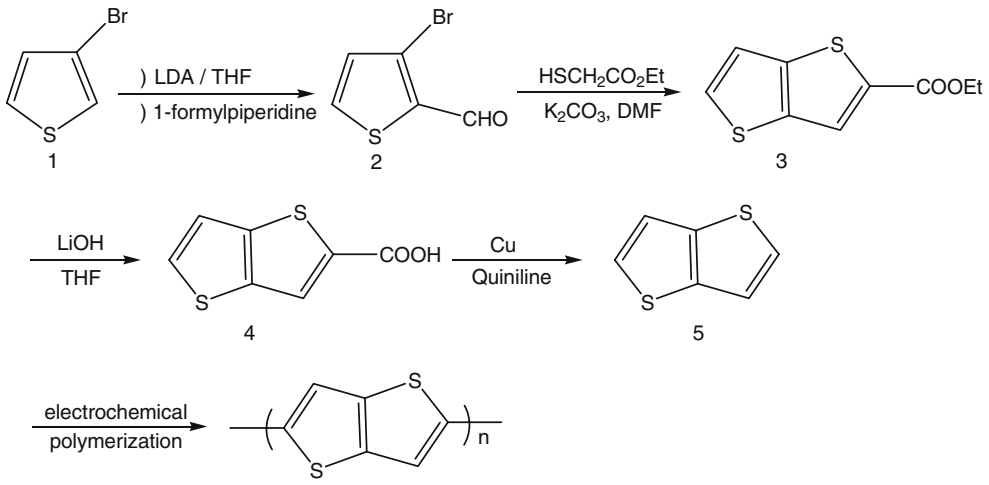

Scheme 1 Synthetic route of PTT

with a diameter of 0.5 mm, respectively, and placed 0.5 cm apart. Before each examination, they were carefully polished and cleaned with water and acetone successively. An Ag/AgCl electrode immersed directly in the solution was used as the reference electrode. A correction of 0.069 V is needed to bring the measured potentials in BFEE originally vs. Ag/AgCl to potentials vs. the standard hydrogen electrode [48]. To obtain a sufficient amount of polymer, a platinum sheet with a surface area of 4.5 cm^2 and a stainless steel sheet with a surface area of 5.0 cm^2 were employed as the working and counter-electrodes, respectively, and they were carefully polished with abrasive paper (1500 mesh) and then washed with water and acetone successively before each examination. The polymers deposited on indium tin oxide (ITO) glasses (about 2.0 cm^2) were used for ultraviolet–visible (UV–visible) measurements and scanning electron microscopy images.

All solutions were deaerated by a dry argon stream before the experiments. For a special analysis, the as-formed polymers were de-doped with 25% ammonium for 3 days and then washed repeatedly with water and acetone. Lastly, they were dried at 60 °C for 2 days in vacuum.

Measurements and characterization

The temperature dependence of both electrical conductivity (σ) and Seebeck coefficient (S) were measured by a four-point measurement unit of thermoelectric properties coupled with a liquid nitrogen container for rectangular-shaped film samples (length, 12.0 mm; width, 4.0 mm; thickness, 0.10 mm) at temperatures from room temperature to 100 K. Cu (99.9%) wires as electrodes and the thermocouples were bound to a sample with conductive paste. When constant DC current was applied between Cu electrodes placed in both edges of a sample across the length, potential drop was detected between Cu wires of the thermocouples placed on the center of the sample surface with a certain distance. Electrical conductivity was determined with the potential drop, the applied current, and sample dimensions. Seebeck coefficient was obtained from the slope of the produced thermoelectric voltage as a function of the temperature difference along the length of the sample. The power factor ($P = S^2\sigma$) was calculated from the corresponding Seebeck coefficient and electrical conductivity at a certain temperature.

UV–visible spectra were measured with a Perkin-Elmer Lambda 900 UV–visible–near-infrared spectrophotometer. Infrared spectra were recorded with a Bruker Vertex 70 Fourier transform infrared (FT-IR) spectrometer with samples in KBr pellets. Thermogravimetric analysis was performed with a Pyris Diamond TG/DTA thermal analyzer (Perkin-Elmer). A VEGA\\LSU TESCAN scanning electron microscope was used to analyze the surface morphologies of the as-formed polymer films.

Results and discussion

Electrochemical polymerization of TT

Figure 1 shows the anodic polarization curves of 0.02 mol L^{-1} TT in BFEE (a), ACN (b), and CH_2Cl_2 (c) solutions. The onset oxidation potential of TT in BFEE was about 0.62 V, which was much lower than those in ACN (1.32 V) and CH_2Cl_2 (1.35 V) solutions. This can be attributed to the interaction between the middle strong Lewis acid BFEE and the aromatic monomer (coordination between the sulfur atom of the monomer and BF_3), which decreases the aromaticity of the fused rings and has a catalytic effect on the electropolymerization of the aromatic monomer [49, 50]. The above condition indicates that the oxidation and polymerization of TT in BFEE is much easier

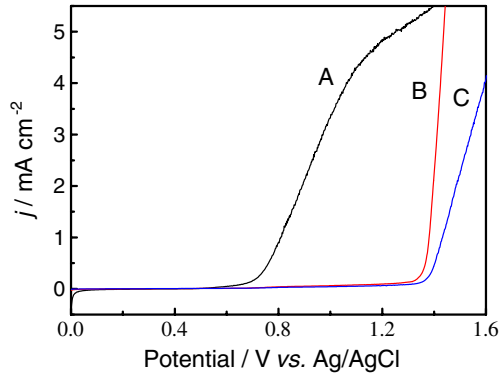

Fig. 1 Anodic polarization curves of 0.02 mol L^{-1} TT in **a** BFEE, **b** ACN + 0.1 mol L^{-1} Bu_4NBF_4, and **c** CH_2Cl_2 + 0.1 mol L^{-1} Bu_4NBF_4 solutions. Potential scan rate, 20 mV s^{-1}

than those in ACN and CH_2Cl_2 solutions. Based on these results, BFEE may be the better electrolyte for the electropolymerization of TT with less side reactions, affording higher-quality polymer films. Moreover, the onset oxidation potential of TT in BFEE (0.62 V) is also lower than that of thiophene (1.10 V vs. Ag/AgCl) recorded in a similar medium [17], which can be ascribed to the extended π-conjugated structure of the TT molecule.

The successive cyclic voltammograms (CVs) of 0.02 mol L^{-1} TT in BFEE (a), ACN (b), and CH_2Cl_2 (c) solutions on a Pt wire electrode, respectively, are shown in Fig. 2. As the CV scanning continued, conducting polymer films were formed on the working electrode surface as observed by visual observation. The increase in the redox wave current densities implied that the amount of conducting polymer deposited on the working electrode was increased. Moreover, the broad redox waves of the as-formed polymer films were attributed to the wide distribution of the polymer or oligomer chain length [51] or the conversion of conductive species on the polymer main chain from the neutral state to polarons, from polarons to bipolarons, and finally from bipolarons to the conductive state [52]. For the CVs recorded in BFEE (Fig. 2a), redox waves can be found at 0.53 V and −0.10 V. Wider reduction waves can be seen at 0.80 V in the CVs recorded in ACN (Fig. 2b) and CH_2Cl_2 (Fig. 2c) solutions, while the oxidation waves were unobvious for these CVs, especially for the CVs recorded in the CH_2Cl_2 solution, revealing bad reversibility. In comparison, the electroactivity and the reversibility of the electron transfer during the electropolymerization of TT in BFEE was better than those in ACN and CH_2Cl_2 solutions. The slight potential shift of the wave current density maximum on the CVs provided information on the increase in the electrical resistance of the polymer films, and higher potentials were needed to overcome the resistance [53]. Furthermore, as the first circle of each CVs presented in different colors shown, TT in BFEE, ACN, and CH_2Cl_2 solutions can be initially oxidized at 0.61 V, 1.36 V, and 1.35 V, respectively, similar with those recorded in Fig. 1. The minute differences between the two groups of data are reasonable and acceptable, suggesting good stability of the systems and fine repeatability of the electrochemical experiments, and they can be caused by surrounding temperature, air humidity, and even parallax reading error.

Electrochemistry of PTT films

The electrochemical behaviors of PTT films deposited in BFEE (Fig. 3a, b), ACN (Fig. 3c, d), and CH_2Cl_2 (Fig. 3e, f) solutions were tested in monomer-free BFEE (Fig. 3a), ACN (Fig. 3c), CH_2Cl_2 (Fig. 3e), and concentrated sulfuric acid (Fig. 3b, d, f), respectively. Similar to the results reported previously [54–57], these CVs represented broad anodic and

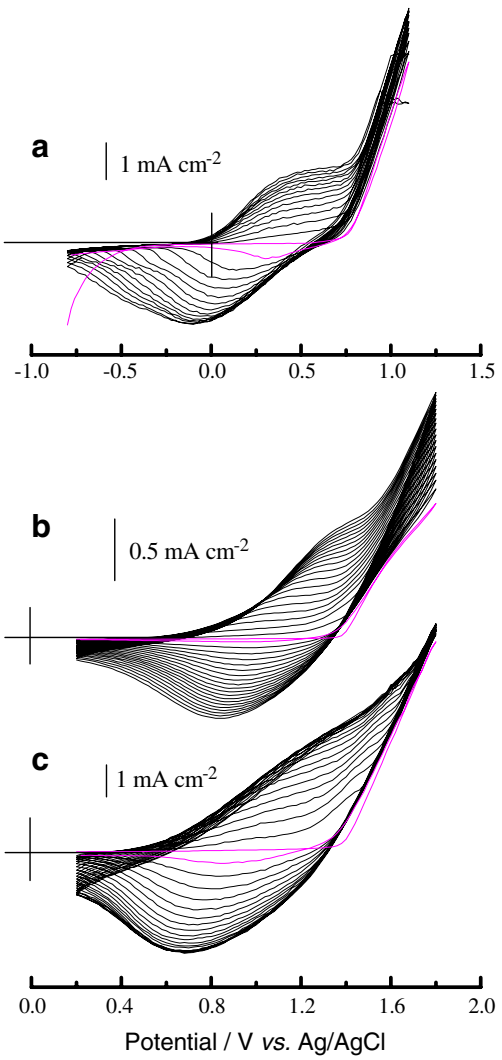

Fig. 2 Cyclic voltammograms of 0.02 mol L^{-1} TT in **a** BFEE, **b** ACN + 0.1 mol L^{-1} Bu_4NBF_4, and **c** CH_2Cl_2 + 0.1 mol L^{-1} Bu_4NBF_4 solutions. Potential scan rate, 100 mV s^{-1}

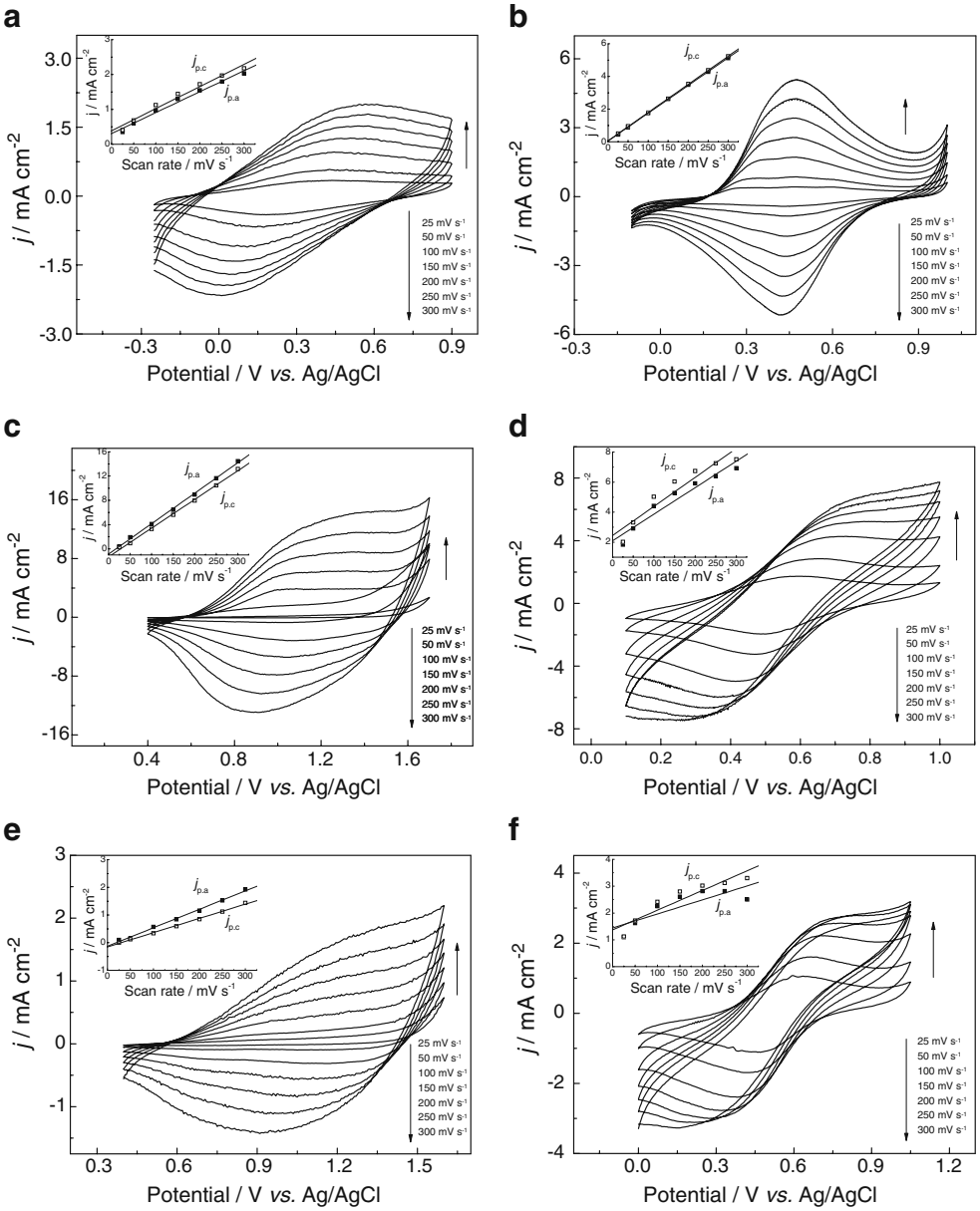

Fig. 3 Cyclic voltammograms of PTT films recorded in monomer-free **a** BFEE, **c** ACN + 0.1 mol L^{-1} Bu_4NBF_4, **e** CH_2Cl_2 + 0.1 mol L^{-1} Bu_4NBF_4, and **b**, **d**, **f** concentrated sulfuric acid at different potential scan rates, respectively. These PTT films were deposited in **a**, **b** BFEE, **c**, **d** ACN + 0.1 mol L^{-1} Bu_4NBF_4, and **e**, **f** CH_2Cl_2 + 0.1 mol L^{-1} Bu_4NBF_4 solutions at constant potentials of 0.80, 1.40, and 1.45 V vs. Ag/AgCl, respectively. j, $j_{p.a}$, and $j_{p.c}$ are defined as current density, anodic peak current density, and cathodic peak current density, respectively

cathodic peaks, which might be attributed to the coupling defects distributed statistically during the electropolymerization process, resulting in the wide distribution of the polymer chain length [51]. For PTT films deposited in BFEE, it could be oxidized and reduced from 0.55 V (anodic peak potential, E_a) to 0 V (cathodic peak potential, E_c) in monomer-free BFEE (Fig. 3a) and from 0.47 V (E_a) to 0.42 V (E_c) in concentrated sulfuric acid (Fig. 3b). The ratio of E_a/E_c was determined to be close to 1 in concentrated sulfuric acid and the peak current densities at the constant potential scan rate were almost the same, which might suggest the good redox activity and reversible doping/dedoping process of the PTT films. Similar results can also be found in the CVs recorded in monomer-free ACN (Fig. 3c), CH_2Cl_2 (Fig. 3e), and concentrated sulfuric acid (Fig. 3d, f). For PTT that deposited from BFEE, obvious reversible voltammetry can be observed in the monomer-free solution in comparison to the case of CH_2Cl_2 and ACN, which may be attributed to the high-quality PTT films and the more facile counter-ion diffusion in BFEE solution. In BFEE, the oxidation potentials of aromatic monomers are usually much lower than those recorded in common neutral or strongly acidic solvents, which will not initiate the over-oxidation and additive polymerization of the monomer. As a result, a high-quality polymer film with good mechanical and conductive properties is obtained, which will contribute to its reversible performance during cyclic voltammetry experiments. On the other hand, BFEE can exist in diethyl ether as a polar molecule, $\left[(C_2H_5)_3O^+\right]BF_4^-$, which furnishes a conducting medium, and the ion conductivity of BFEE can be up to

2.97×10^{-4}S cm^{-1} at 25°C, which will be beneficial to the diffusion of counter-ion between the solution and the polymer film. As the oxidation/reduction process of the polymer film is related to the counter-ion in/out of the conducting film, therefore, the more facile counter-ion diffusion in BFEE solution properly contributes to the reversible cyclic voltammetry performance. On the whole, all as-formed PTT films could be cycled repeatedly between conducting (oxidized) and insulating (neutral) states, without a significant decomposition of the material in corresponding monomer-free solutions, implying high redox activity and stability of the PTT films. A summary of the oxidation and reduction potentials of these polymer films in different electrolytes is listed in Table 1.

From the insets in Fig. 3, a linear dependence between current density and potential scan rate can be clearly observed in Fig. 3a, b, c, e, suggesting good redox reversibility and high electrochemical activity of PTT films in corresponding media. While the CVs of PTT films deposited from CH_2Cl_2 and ACN media recorded in monomer-free concentrated sulfuric acid (Fig. 3d, f), the peak current density increased slowly rather than proportionally as the potential scan rate increased from 25 to 300 mV s^{-1}, and no linear dependence between them was found, especially for that in Fig. 3f. This can be attributed to that in CH_2Cl_2 and ACN media; TT exhibited a higher onset oxidation potential (1.35 and 1.32 V, respectively) compared with that in BFEE (0.62 V), which may easily cause the over-oxidation of the monomer or oligomer and, subsequently, impact on the regularity of the π-conjugated chain structure and/or polymer chain packing. The above condition will cause bad electrochemical stability, low conducting property, and redox irreversibility of the polymer films in concentrated sulfuric acid. Moreover, the doped ions BF_4^- diffusion between film and solution may also have contributions to the defective voltammetry performance of PTT film in concentrated sulfuric acid.

It is well known that good stability of conducting polymer films is needed to their applications in electronic devices [58]. Therefore, the long-term stability of the redox activity of the PTT film prepared from BFEE was also investigated in monomer-free BFEE (Fig. 4). The extended CVs were recorded between 0.90 and −0.25 V for 200 cycles, at a potential scan rate of 100 mV s^{-1}. The as-formed PTT film could be cycled repeatedly between the conducting (oxidized) and insulating (neutral) states without significant decomposition, indicating high redox activity and stability of PTT films.

Structural characterization

Similar with PT, the solubility of PTT films prepared from BFEE, ACN, and CH_2Cl_2 solutions were bad and they hardly dissolve in most common organic solvents, such as ethanol, acetone, dimethyl sulfoxide (DMSO), ethyl ether, chloroform, DMF, and THF. The UV–vis spectra of PTT films deposited on ITO glasses potentiostatically in BFEE (a), ACN (b), and CH_2Cl_2 (c) solutions were shown in Fig. 5. The absorption of monomer TT dissolved in DMSO (inset of Fig. 5) showed a characteristic absorption at about 350 nm, which was assigned the π–π* transition of thienyl rings. As shown in Fig. 5, all the absorption spectra of PTT films synthesized in BFEE, ACN, and CH_2Cl_2 systems showed broad and strong absorptions from 366 to 616 nm, with a maximum absorption at about 475 nm, reflecting the enhanced π-conjugated region and the wide distribution of the length of the polymer main chains. Consequently, the absorption peaks of PTT performed greatly red-shift compared with that of the monomer TT. These results confirmed the formation of a new conjugated conducting polymer.

Figure 6 shows the FT-IR spectra of TT monomer (a) and PTT electrodeposited from BFEE (b), ACN (c), and CH_2Cl_2 (d) in de-doped state. As the spectrum of TT shown (a), the bands at 3,122, 924, 875, 777, and 680 cm^{-1} were assigned to stretching modes and deformation vibrations of C–H in the thiophene rings [14, 15], and the corresponding bands at 3,130 and 785 cm^{-1} could be observed in the spectra of PTT (b–d). The bands at 1,616, 1,412, and 1,347 cm^{-1} originated to the stretching modes of C=C and

Table 1 Redox peak potentials of the CVs of PTT films electrodeposited in BFEE, ACN + 0.1 mol L^{-1} Bu_4NBF_4, and CH_2Cl_2 + 0.1 mol L^{-1} Bu_4NBF_4 solutions potentiostatically. The CVs were recorded in monomer-free BFEE, ACN + 0.1 mol L^{-1} Bu_4NBF_4, CH_2Cl_2 + 0.1 mol L^{-1} Bu_4NBF_4, and concentrated sulfuric acid, respectively. All the potentials were versus Ag/AgCl

	BFEE		ACN + Bu_4NBF_4		CH_2Cl_2 + Bu_4NBF_4		Concentrated sulfuric acid	
	E_{pa}	E_{pc}	E_{pa}	E_{pc}	E_{pa}	E_{pc}	E_{pa}	E_{pc}
PTT (BFEE)	0.48	0.02					0.47	0.45
PTT (ACN)			1.20	0.93			0.70	0.40
PTT (CH_2Cl_2)					1.30	0.94	0.73	0.38

E_{pa} anodic peak potential (V), E_{pc} cathodic peak potential (V)

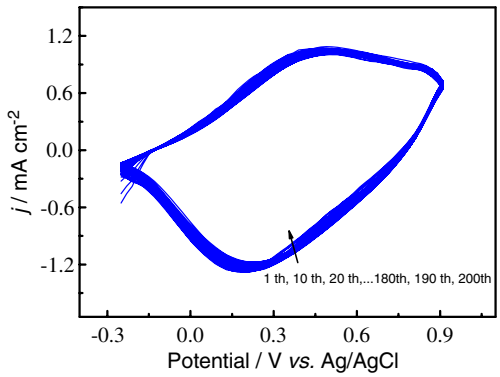

Fig. 4 Extended CVs of PTT film recorded in monomer-free BFEE at the potential scan rate of 100 mV s^{-1}. Selected cycles are presented as indicated. The film was electrodeposited in BFEE at an applied potential of 0.80 V vs. Ag/AgCl. *j* was defined as current density

C–C, and the band at 680 cm^{-1} was assigned to the stretching vibration of C–S–C. For the polymers, corresponding vibration bands at higher or lower wave numbers (1,625, 1,404, 1,138, 1,090, and 638 cm^{-1}) were observed (b–d). After polymerization, some vibration bands disappeared in the spectra of PTT compared with that of TT monomer, and the PTT samples synthesized from different systems showed very similar FT-IR spectra (b–d), indicating the similar composition of the samples.

Thermoelectric property

In BFEE solution, free-standing PTT films could be directly peeled off from the working electrode surface by hand and also could be cut into kinds of shapes with a pair of scissors (Fig. 7). The temperature dependence of electrical conductivity (σ) and Seebeck coefficient (*S*) of these free-standing PTT films were measured, as shown in Fig. 8. For PTT films electrodeposited from ACN and CH_2Cl_2 solutions, they were both so brittle that were hard to form free-standing films and it was also difficult to press the crushed PTT powder into pellets. Thus, the thermoelectric measurements for PTT synthesized from ACN and CH_2Cl_2 systems suffered a failure.

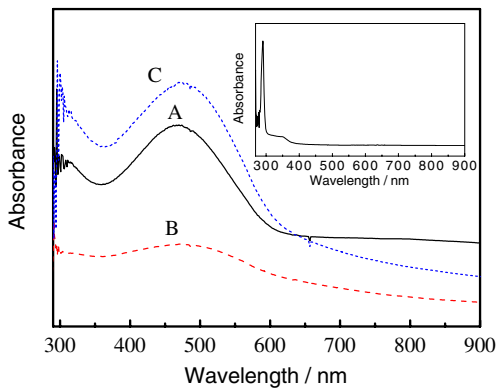

Fig. 5 UV–vis spectra of de-doped PTT films deposited on ITO glasses from **a** BFEE, **b** ACN + 0.1 mol L^{-1} Bu_4NBF_4, and **c** CH_2Cl_2 + 0.1 mol L^{-1} Bu_4NBF_4 solutions, respectively. *Inset*, UV–vis spectrum of TT in DMSO

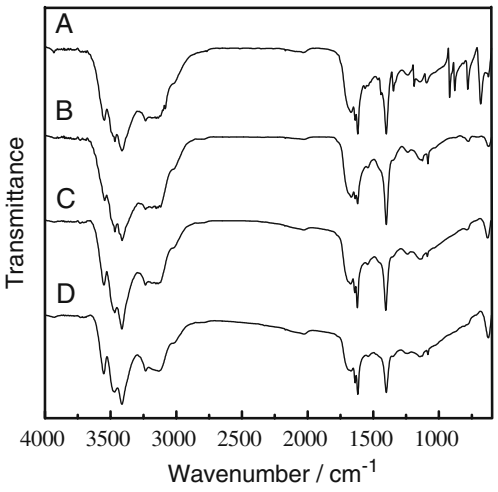

Fig. 6 FT-IR spectra of **a** TT and PTT electrosynthesized from **b** BFEE, **c** ACN + 0.1 mol L^{-1} Bu_4NBF_4, and **d** CH_2Cl_2 + 0.1 mol L^{-1} Bu_4NBF_4 solutions in de-doped state

As shown in Fig. 8, the electrical conductivity of PTT films was 1.5 Scm^{-1} at 306 K, much higher than that reported previously [12, 15]. With a decrease in the temperature, the electrical conductivity decreased gradually, a typical behavior of semiconductors [40–46, 59–61]. From 306 to 200 K, the electrical conductivity took a much rapid decrease in speed, and it slowed down when below 200 K. When the temperature reached 100 K, the electrical conductivity decreased to 0.02 Scm^{-1}. Similar with electrical conductivity, the Seebeck coefficient of PTT films decreased gradually as the temperature decreased (Fig. 8). At 306 K, the Seebeck coefficient of PTT films could be up to 85 $\mu V K^{-1}$, and when the temperature decreased to 140 K

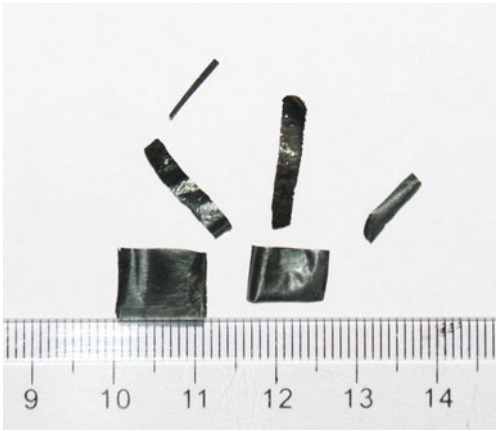

Fig. 7 Photograph of free-standing conducting PTT films prepared from BFEE at the constant applied potential of 0.80 V vs. Ag/AgCl

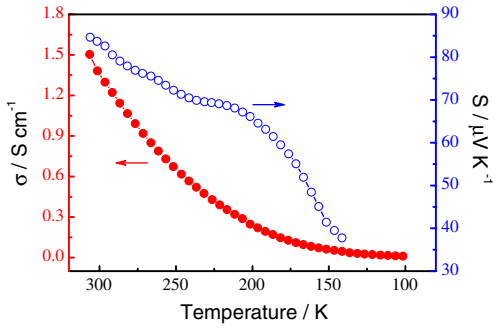

Fig. 8 Temperature dependence of electrical conductivity σ and Seebeck coefficient S for PTT films electrodeposited from BFEE at the constant applied potential of 0.80 V vs. Ag/AgCl

it correspondingly decreased to 38 μV K^{-1}. The Seebeck coefficient is positive, indicating that the charge carriers are holes [62]. By comparison with the thermoelectric properties of PT and poly(3-methylthiophene) (PMeT) films [59], the Seebeck coefficients of PTT films are higher than those of PT (28-43 μV K^{-1}) and PMeT films (18-31 μV K^{-1}) at corresponding temperatures. However, the measured electrical conductivities of PTT films are much lower than those of PT and PMeT films [59], possibly because of the low purity of TT monomer, the relatively rougher film surface, or the polymerization conditions of the system and the surroundings. Therefore, further studies aiming to improve the electrical conductivity of PTT films are quite essential in the future research on PTT.

Figure 9 shows the temperature dependence of power factor P ($=S^2\sigma$) and the estimated dimensionless figure-of-merit ZT values of PTT films. The power factor of PTT films was 1.1 μW $m^{-1}K^{-2}$ at 306 K. Since the power factor is proportional to the square of the Seebeck coefficient and the electrical conductivity, thus the power factor decreased as the temperature decreased. Obviously, the thermoelectric property of PTT films is much sensitive to the temperature.

The dimensionless figure-of-merit ZT values of PTT films have not been calculated because the thermal conductivity measurement process of one material is complicated and the thermal conductivity (κ) of PTT films has not yet been evaluated. However, as the literature reported, the differences between the thermal conductivities (κ) of most organic thermoelectric materials are usually very little, such as polyaniline (κ, 0.02–0.15 W $m^{-1}K^{-1}$; T, 300 K; different doping level) [60], PEDOT:PSS (κ, 0.04–0.17 $Wm^{-1}K^{-1}$; T, 150–290 K) [61], PT (κ, 0.03–0.17 $Wm^{-1}K^{-1}$; T, 100–320 K) [59], and PMeT (κ, 0.02–0.15 $Wm^{-1}K^{-1}$; T, 100–320 K) [59]. Considering the similar molecule structures of PTT with PT and the little differences between the thermal conductivities of most organic thermoelectric materials, we estimated the ZT values of PTT films based on the thermal conductivities of PT films. As shown in Fig. 9, the ZT value of PTT at 306 K was 2.3×10^{-3} and it slightly decreased to 2.2×10^{-3} when the temperature decreased to 280 K; as the temperature continuously decreased to 266 K, the ZT value increased slowly to the maximum value of 2.5×10^{-3}, which was higher than those of PEDOT:PSS pellets (1.75×10^{-3}) [61] and polyaniline films (1×10^{-4}) [63]. Then, the ZT values decreased again as the temperature continued to decrease. The difference between the thermoelectric performances of PTT films and inorganic thermoelectric materials such as β-$FeSi_2$ (Z, ca. 2×10^{-4} K^{-1}; ZT, 6×10^{-2}) [64] is not so much that some more intensive study can be done to narrow the gap between them.

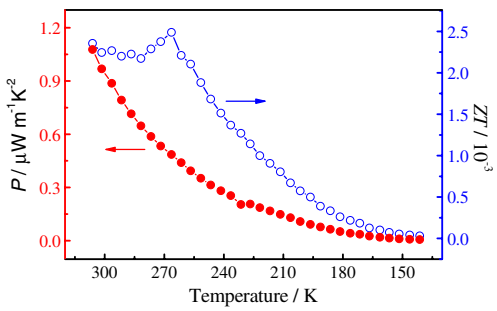

Fig. 9 Temperature dependence of power factor P and estimated ZT values for PTT film electrodeposited from BFEE at 0.80 V vs. Ag/AgCl potentiostatically

Thermal property

For conducting polymers, thermal stability is very important for their potential applications. To investigate the thermal stability of PTT, thermogravimetric analytical experiments were carried out under a nitrogen stream at

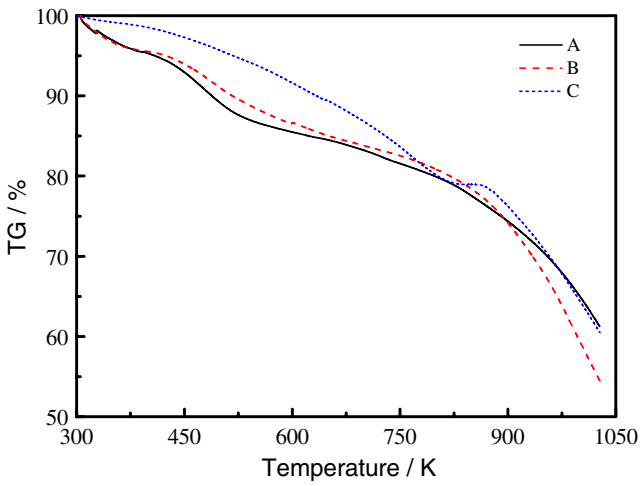

Fig. 10 Thermogravimetric (TG) curves of PTT films in doped state prepared from **a** BFEE, **b** ACN + 0.1 mol L^{-1} Bu_4NBF_4, and **c** CH_2Cl_2 + 0.1 mol L^{-1} Bu_4NBF_4 potentiostatically

a heating rate of 10 Kmin^{-1}. Figure 10 shows the thermal properties of PTT films in doped state electropolymerized from BFEE (a), ACN (b), and CH_2Cl_2 (c) solutions, respectively. The heat-degradation behavior of PTT films from BFEE (a) was similar with that from ACN (b). From 300 to 396 K, they both went through a mass loss of 5%, mainly because of some water or moisture trapped into the polymer matrices. From 396 to 565 K, they got another weight loss of 10% and this was caused by the degradation of the oligomers. When the temperature reached 800 K, a serious mass loss happened to them, which indicated the decomposition of the skeletal PTT main chain structure. For PTT electrodeposited in CH_2Cl_2 (C) solution, it initially went through a slow degradation of about 21% as the temperature increased from 300 to 820 K, and this might be attributed to the degradation of the oligomers obtained during the polymerization process. When the temperature reached 865 K, a rapid mass loss occurred, revealing the decomposition of the skeletal PTT backbone structure. The above results suggested that the obtained PTT films, no matter if polymerized from BFEE, ACN (b), or CH_2Cl_2 (c) solutions, all exhibited good thermal stability.

Conclusions

In summary, we successfully synthesized TT monomer and electrosynthesized PTT films from BFEE, ACN + 0.1 mol L^{-1} Bu_4NBF_4, and CH_2Cl_2 + 0.1 mol L^{-1} Bu_4NBF_4 solutions, respectively. By comparison, the PTT films prepared from BFEE exhibited better electrochemical property, higher structure, and thermal stability. In BFEE solution, free-standing PTT films with good mechanical property could be easily peeled off from the electrode surface by hand. Moreover, the as-formed free-standing PTT films with an electrical conductivity of 1.5 Scm^{-1} and a Seebeck coefficient of 85 μV K^{-1} at ambient temperature showed a good thermoelectric property. The Seebeck coefficient of PTT film is higher than those of PT and PMeT films, but the electrical conductivity of PTT film is much lower than those of PT and PMeT films, and much intensive studies should be done to further analyze and improve the electrical property of the PTT film. The calculated power factor *P* and the estimated *ZT* value of PTT films were 1.1 μW $m^{-1}K^{-2}$ and 2.3×10^{-3} at 306 K, respectively, higher than those of some organic thermoelectric materials reported previously. Therefore, PTT films may have potential application as one novel organic thermoelectric material.

Acknowledgements NSFC (50663001, 50963002) and Jiangxi Province Jinggang Star Project (2008) are acknowledged for their financial supports.

References

1. Shirakawa H, Louis EJ, MacDiarmid AG, Chiang CK, Heeger AJ (1977) J Chem Soc Chem Commun 16:578
2. Chiang CK, Fincher CR, Park YW, Heeger AJ, Shirakawa H, Louis EJ, Gau SC, MacDiarmid AG (1977) Phys ReV Lett 39:1098
3. Skotheim TA, Reynolds JR (2007) Handbook of conducting polymers (chap. 15-22), 3rd edn. CRC, Boca Raton
4. Xiao K, Liu YQ, Qi T, Zhang W, Wang F, Gao JH, Qiu WF, Ma YQ, Cui GL, Chen SY, Zhan XW, Yu G, Qin JG, Hu WP, Zhu DB (2005) J Am Chem Soc 127:13281
5. Okamoto T, Kudoh K, Wakamiya A, Yamaguchi S (2005) Org Lett 7:5301
6. Murphy AR, Frechet JM (2007) J Chem Rev 107:1066
7. Cremer LD, Verbiest T, Koeckelberghs G (2008) Macromolecules 41:568
8. Jung SH, Kim HK, Kim SH, Kim YH, Jeoung SC, Kim D (2000) Macromolecules 33:9277
9. Lim E, Jung BJ, Shim HK (2003) Macromolecules 36:4288
10. Kim HS, Kim YH, Kim TH, Noh YY, Pyo S, Yi MH, Kim DY, Kwon SK (2007) Chem Mater 19:3561
11. Chen MC, Chiang YJ, Kim C, Guo YJ, Chen SY, Liang YJ, Huang YW, Hu TS, Lee GH, Facchettib A, Marksbm TJ (2009) Chem Commun 14:1846
12. Danieli R, Taliani C, Zamboni R, Giro G, Biserni M, Mastragostino M, Testoni A (1986) Synth Met 13:325
13. Taliani C, Danieli R, Zamboni R, Ostoja P, Poraio W (1987) Synth Met 18:177
14. Yang L, Dorsinville R, Wang QZ, Zou WK, Ho PP, Yang NL, Alfano RR, Zamboni R, Danieli R, Ruani G, Taliani C (1989) J Opt Soc Am B 6:753
15. Taliani C, Zamboni R, Danieli R, Ostoja P, Porzio W, Lazzaroni R, Bredas JL (1989) Phys Scr 40:781
16. Gurunathan K, VadivelMurugan A, Marimuthu R, Mulik UP, Amalnerkar DP (1999) Mater Chem Phys 61:173
17. Shi GQ, Jin S, Xue G, Li C (1995) Science 267:994
18. Shi GQ, Li C, Liang YQ (1999) Adv Mater 11:1145
19. Li C, Shi GQ, Liang YQ (1998) J Electroanal Chem 455:1
20. Huang ZM, Qu LT, Shi GQ, Chen FE, Hong XY (2003) J Electroanal Chem 556:159
21. Li C, Shi GQ, Liang YQ, Ye W, Sha Z (1997) Polymer 38:5023
22. Wang XB, Shi GQ, Liang YQ (1999) Electrochem Commun 1:536
23. Zoski CG (2007) Handbook of electrochemistry. Elsevier press, Amsterdam
24. Heeger AJ (2001) J Phys Chem 105:8475
25. MacDiarmid AG (2002) Synth Met 125:11
26. Kraft A, Grimsdale AC, Holmes AB (1998) Angew Chem Int Ed 37:402
27. Dimitrakopoulos CD, Malenfant PR (2001) Adv Mater 14:99
28. Winder C, Sariciftci NS (2004) J Mater Chem 14:1077
29. Yan H, Toshima N (1999) Chem Lett 28:1217
30. Yan H, Ohno N, Toshima N (2000) Chem Lett 29:392
31. Yan H, Ohta T, Toshima N (2001) Macromol Mater Eng 286:214
32. Shinohara Y, Hiraishi K, Nakanishi H, Isoda Y, Imai Y (2005) Trans Mater Res Soc Jpn 30:963
33. Shinohara Y, Ohara K, Imai Y, Isoda Y, Nakanishi H (2004) Trans Mater Res Soc Jpn 29:1921
34. Hu E, Kaynak A, Li Y (2005) Synth Met 150:139
35. Yim B, Rosi F (1972) Solid-State Electron 15:1121
36. Deng Y, Nan CW, Guo L (2004) Chem Phys Lett 5/6:572
37. Deng Y, Cui CW, Zhang NL, Ji TH, Yang QL, Gou L (2006) J Solid State Chem 5:1575
38. Deng Y, Nan CW, Wei GD, Guo L, Lin YH (2003) Chem Phys Lett 3/4:410

39. Deng Y, Cui CW, Zhang NL, Ji TH, Yang QL, Guo L (2006) Solid State Commun 3:111
40. Hiroshige Y, Ookawa M, Toshima N (2006) Synth Met 156:1341
41. Hiroshige Y, Ookawa M, Toshima N (2007) Synth Met 157:467
42. Lévesque I, Gao X, Klug DD, Tse JS, Ratcliffe CI, Leclerc M (2005) React Funct Polym 65:23
43. Aïch RB, Blouin N, Bouchard A, Leclerc M (2009) Chem Mater 21:751
44. Lévesque I, Bertrand PO, Blouin N, Leclerc M, Zecchin S, Zotti G, Ratcliffe CI, Klug DD, Gao X, Gao FM, Tse JS (2007) Chem Mater 19:2128
45. Pintér E, Fekete ZA, Berkesi O, Makra P, Patzkó Á, Visy C (2007) J Phys Chem C 111:11872
46. Kim JY, Jung JH, Lee DE, Joo J (2002) Synth Met 126:311
47. Fuller LS, Iddon B, Smith KA (1997) J Chem Soc Perkin Trans 1:3465
48. Game RR, Allison JL, Call RS, Coval CA (1977) J Am Chem Soc 99:7170
49. Chen W, Xue G (2005) Prog Polym Sci 30:811
50. Jin S, Xue G (1997) Macromolecules 30:5753
51. Zhou M, Heinze J (1999) Electrochim Acta 44:1733
52. Lu BY, Xu JK, Fan CL, Jiang FX, Miao HM (2008) Electrochim Acta 54:334
53. Otero TF, Larreta-Azelain ED (1988) Polymer 29:1522
54. Yue RR, Xu JK, Lu BY, Liu CC, Li YZ, Zhu ZJ, Chen S (2009) J Mater Sci 44:5909
55. Zhang C, Xu Y, Wang NC, Xu Y, Xiang WQ, Ouyang M, Ma CN (2009) Electrochim Acta 55:13
56. Nie GM, Cai T, Zhang SS, Bao Q, Xu JK (2007) Electrochim Acta 52:7097
57. Xu JK, Wei ZH, Du YK, Zhou WQ, Pu SZ (2006) Electrochim Acta 51:4771
58. Uckert F, Tak YH, Müllen K, Bässler H (2000) Adv Mater 12:905
59. Lu BY, Liu CC, Lu S, Xu JK, Jiang FX, Zhang Z (2010) Chin Phys Lett 27:057201
60. Yan H, Sada N, Toshima N (2002) J Therm Anal Calorim 69:881
61. Jiang FX, Xu JK, Lu BY, Xie Y, Huang RJ, Li LF (2008) Chin Phys Lett 25:2202
62. Masubushi S, Kazama S, Mizoguchi K, Honda M, Kume K, Matsushita R, Matsuyama T (1993) Synth Met 55:4962
63. Toshima N (2002) Macromol Symp 186:81
64. Birkholtz U, Groβ E, Stöhrer U, Rowe DM (1995) CRC handbook of thermoelectrics. CRC, Boca Raton